Available online at www.sciencedirect.com
SCIENCE DIRECT®
Journal of Power Sources 137 (2004) 175–182
JOURNAL OF POWER SOURCES
www.elsevier.com/locate/jpowsour

Inorganic proton-conducting gel glass/porous alumina nanocomposite

Yong-Il Park [a], Masayuki Nagai [b], Jae-Dong Kim [c], Koichi Kobayashi [a,b,*]

[a] *Kumoh National Institute of Technology, School of Materials and System Engineering, 188 Shinpyung-dong, Gumi, Kyungbuk 730-701, South Korea*
[b] *Advanced Research Center for Energy and Environment, Musashi Institute of Technology, 1-28-1 Tamazutsumi, Setagaya-ku, Tokyo 158-8557, Japan*
[c] *R & D Center, Korea Gas Corporation, 638-1 Il-dong, Ansan, Kyunggi-do 425-790, South Korea*

Received 19 January 2004; accepted 28 March 2004
Available online11 September 2004

Abstract

A novel fast proton-conducting silicophosphate-$HClO_4$ (SiP-$HClO_4$) gel glass and SiP-$HClO_4$–alumina composite are successfully fabricated. The fabricated inorganic composites show good thermal stability and stable conductivity up to 140 °C, which indicates a high proton conductivity of over 2.6×10^{-2} S cm^{-1}. The high conductivity of the composites is attributed to the fast proton-conducting property of the three-dimensional SiP-$HClO_4$ gel glass network which contains both trapped acid ions (ClO_4^-) as a proton donor and strongly hydrogen-bonded hydroxyl groups combined to P–O–Si bonds as proton conduction paths.

Keywords: Proton conductor; Sol–gel; Glass; Fuel cell

1. Introduction

As the most practical fuel cell candidate, proton exchange membrane fuel cells (PEMFC) are receiving attention due to their low operating temperature, non-production of CO_2, and suitability for electric vehicles.

In general, the electrolyte material in a PEMFC must be [1]: (i) easily synthesized from available, low-cost starting materials; (ii) highly water-insoluble and film forming; (iii) highly proton-conducting (>0.01 S cm^{-1}); (iv) chemically stable to acids and free-radicals; (v) not permeable to reactant gases (H_2/O_2); (vi) thermally and hydroelectrically stable at high temperature (>120 °C); and (vii) stable in H_2 fuel cells for 5000 h (for vehicle applications).

A proton exchange membrane (PEM) in a PEMFC is an electronic insulator, but is also an excellent conductor of hydrogen ions. A PEM is used in the form of a 50–200 μm thick film and acts as a gas separator and also as an electrolyte. The electrolyte and electrodes are pressed together to produce a single membrane–electrode assembly (MEA). Membranes developed by DuPont (Nafion^{TM} series) and Dow are most widely used. Both membranes consist of perfluorinated copolymers with sulfonic-acid functionalized side-chains. These materials are, however, practical at high temperatures (over 120 °C) and have complicated synthetic procedures [2–8].

To obtain high proton-conducting PEM materials that have also high thermal stability, we have investigated the fabrication of new types of proton-conducting inorganic composites that consist of gel glass and alumina. Glasses are suitable materials for applications that require high thermal stability, mechanical strength, visible transparency, and film formation. Protons in oxide glasses usually remain as X–OH groups (X = Si, P, etc.) in a glass structure when glasses are prepared via a melting process in ambient atmosphere [9–11], while a significant contribution of residual P–OH groups to electrical conduction is observed in phosphate glasses [12]. Hosono et al. [13] showed that protons are the main charge carriers in phosphate glasses. The proton conductivity in phosphate glasses fabricated by a melting process is, however, very low (<10^{-11} S cm^{-1}) because of a low proton carrier density of about 1 mol L^{-1}. Sol–gel derived alkaline phosphate glasses have been developed as fast-proton conducting materials due to their large capacity for hydroxyl groups. Despite the increased proton conductivity, the alkaline phosphate glasses derived from a sol–gel process also have a limit in phosphate concentration due to decreasing mechanical strength and chemical stability with increasing phosphorus concentration [14].

In this study, fast proton-conducting phosphate glasses have high proton density have been fabricated by incorporating perchloric acid in silicophosphate gel glasses

* Corresponding author. Tel.: +82-54-567-4365; fax: +82-54-467-4478.
E-mail address: yiprk@kumoh.ac.kr (K. Kobayashi).

0378-7753/$ – see front matter © 2004 Published by Elsevier B.V.
doi:10.1016/j.jpowsour.2004.03.047

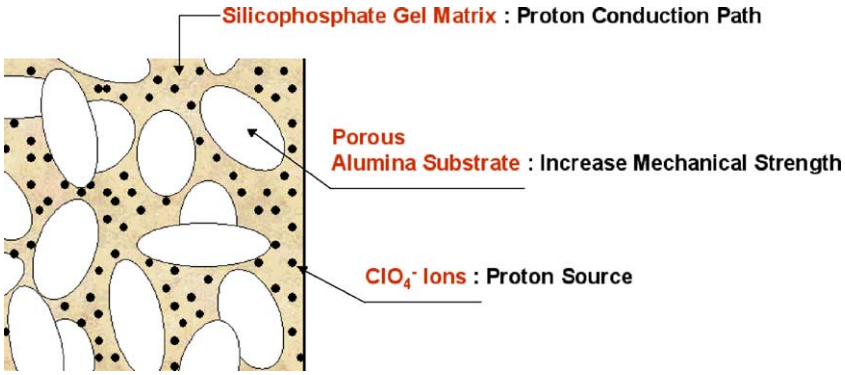

Fig. 1. Schematic diagram of SiP-$HClO_4$–alumina composite.

(SiP-$HClO_4$) through a sol–gel technique. It is difficult, however, to form self-standing thin glass membranes due to cracks caused by the large shrinkage that is inevitable with a sol–gel process. In order to suppress crack formation and to form a self-standing membrane with high mechanical strength, porous sintered alumina is used as a matrix to contain the silicophosphate gel glass (Fig. 1). Through multiple infiltration of the prepared sol into the porous alumina, a proton conduction path is successfully formed in the continuous gel glass phase that fills in the pores of the alumina, and the resulting composite has almost the same conductivity as the SiP-$HClO_4$ gel glass itself.

2. Experimental

2.1. Preparation of precursor solution and gel glass

The SiP-$HClO_4$ precursor solution was prepared by using tetraethoxylsilane (TEOS, $Si(OC_2H_5)_4$, 1 mol), di-isopropyl phosphite ($HPO(OC_3H_7)_2$, 3 mol), and ethanol as starting materials. After 30 min of stirring, 8 mol of $HClO_4$ was added to the starting solution. Then, 1.5 mol of distilled water diluted with ethanol was added to the mixed solution for the hydrolysis reaction. The resulting solution was allowed to gelate for 3 days at 23 °C, 15 RH% and then heat-treated at 100 °C for 2 h to obtain the gel glass sample.

2.2. Preparation of porous alumina

Porous Al_2O_3 substrates were fabricated using commercial fine α-Al_2O_3 powder (Japan Catalytic Chemical Co.) with a surface area of about 150 $m^2\,g^{-1}$. 5 wt.% polyvinylalcohol was added to the powder and it was pressed at 200 $kg\,cm^{-2}$ to form pellets with a diameter of 12 mm and a thickness of 1–2 mm. The pellets were heated at 500 °C, to burn out the binder, and then sintered at 1100 °C for 2 h. The pore-size distribution of the fired samples was determined by the mercury injection method (CARLO ELBA, PO2000).

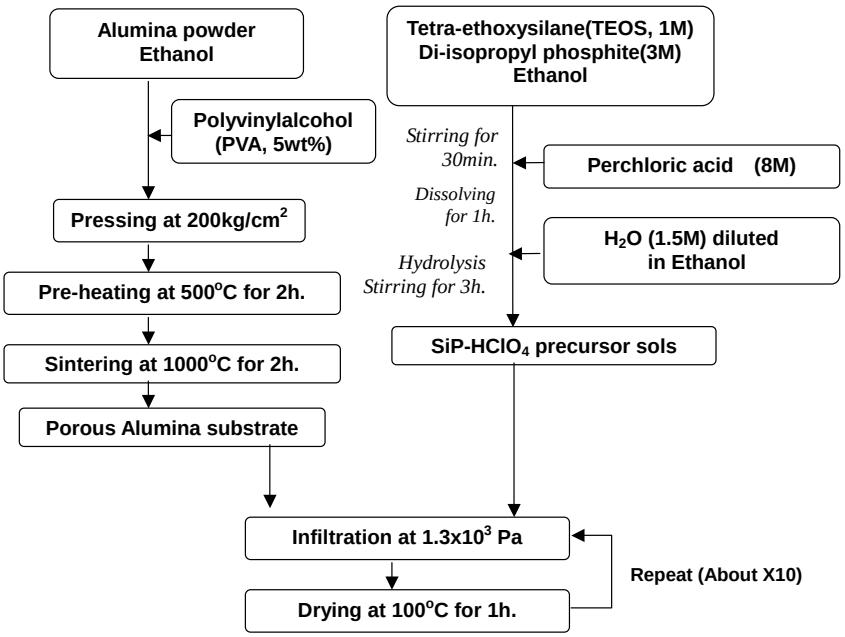

Fig. 2. Flow diagram for fabrication of SiP-$HClO_4$–alumina composite.

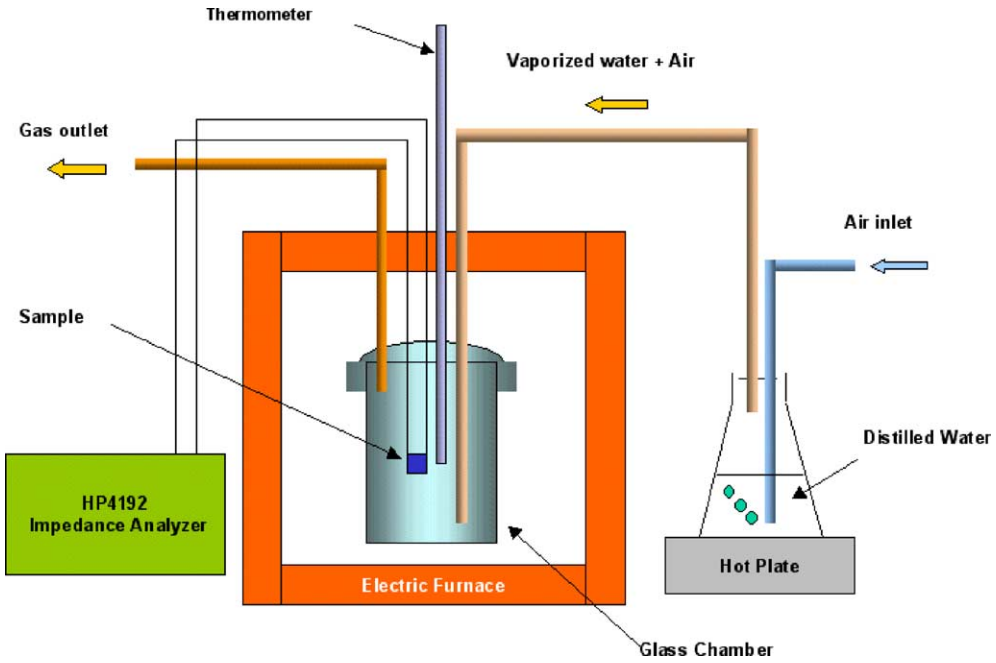

Fig. 3. Experimental set-up for measuring impedance spectra of SiP-$HClO_4$–alumina composite.

2.3. Preparation of composite

Composite samples of the gel glass and alumina were prepared by a multiple infiltration-drying process. Infiltration of SiP-$HClO_4$ precursor solution into the fabricated alumina substrate was carried out under a reduced pressure of 1.3×10^3 Pa, and then the composite sample was heated at 100 °C for 30 min. The infiltration-drying process was repeated until the increase in the weight of the composite ceased. The process is illustrated in Fig. 2.

2.4. Analysis

FT-IR absorption spectra were obtained with a spectrometer (Perkin-Elmer model Spectrum BX) at room temperature to analyze the bond structure of hydroxyl groups and water. A field emission scanning electron microscopy (FE-SEM, Hitachi model S4100) was used to examine the microstructures. Thermogravimetric and differential thermal analysis (TG/DTA) was performed under an ambient atmosphere, using a TG/DTA model 320 instrument (Seiko Electron Co.), and over a temperature range of 20–500 °C. A heating rate of 5 °C min^{-1} was used to analyze the thermal stability. The conductivity of all samples was obtained from Nyquist plots produced by an impedance analyzer (HP4192A impedance Analyzer, Hewlett Packard Co.). The test cells were formed by sandwiching each sample between blocking electrodes of platinum plates. A frequency range of 5 Hz to 13 MHz and a peak-to-peak voltage of 10 mV were used for the impedance measurements. All the test cells were equilibrated for 2 h at each temperature and humidity prior to impedance measurement. Experiments at different relative humidity were performed in a test chamber (ISUZU Co.), and the conductivity at 20–200 °C in ambient atmosphere was measured using the experimental set-up illustrated in Fig. 3.

3. Results and discussion

The fabricated porous alumina has an α-Al_2O_3 phase and a relative density of about 46%. The mean value of the pore size is about 80 nm [15]. The gel glass samples are transparent and rigid, and the composite samples show good mechanical strength and a glassy surface. The SiP-$HClO_4$ gel glass experienced several cracks on the surface during the drying process, which resulted in a breakdown into several pieces.

The fractured surface of the porous alumina substrate is shown in Fig. 4(a). Fractured surfaces of the composite samples after 7 and 10 applications of the infiltration process are shown in Fig. 4(a) and (b), respectively. On repetition of the infiltration process, the pores in the alumina substrate are three-dimensionally filled with SiP-$HClO_4$ gel glass.

The TG/DTA analysis of the dried composite measured in the temperature range from 20 to 500 °C with a heating rate of 5 °C min^{-1} is shown in Fig. 5. A slight exothermic increase is observed at 20–257 °C with an accompanying weight loss. The total weight loss is very small (about 4%), and takes place in two steps. The exothermic increase in the DTA at 20–110 °C is attributed to the accelerated polymerization reaction of the remaining reactant alkyl groups of alkoxides or P–OH groups to form metal–oxygen bonds. The 2% of decrease in TG is due to evaporation of alcohol or water biproduct and adsorbed surface water. The weight

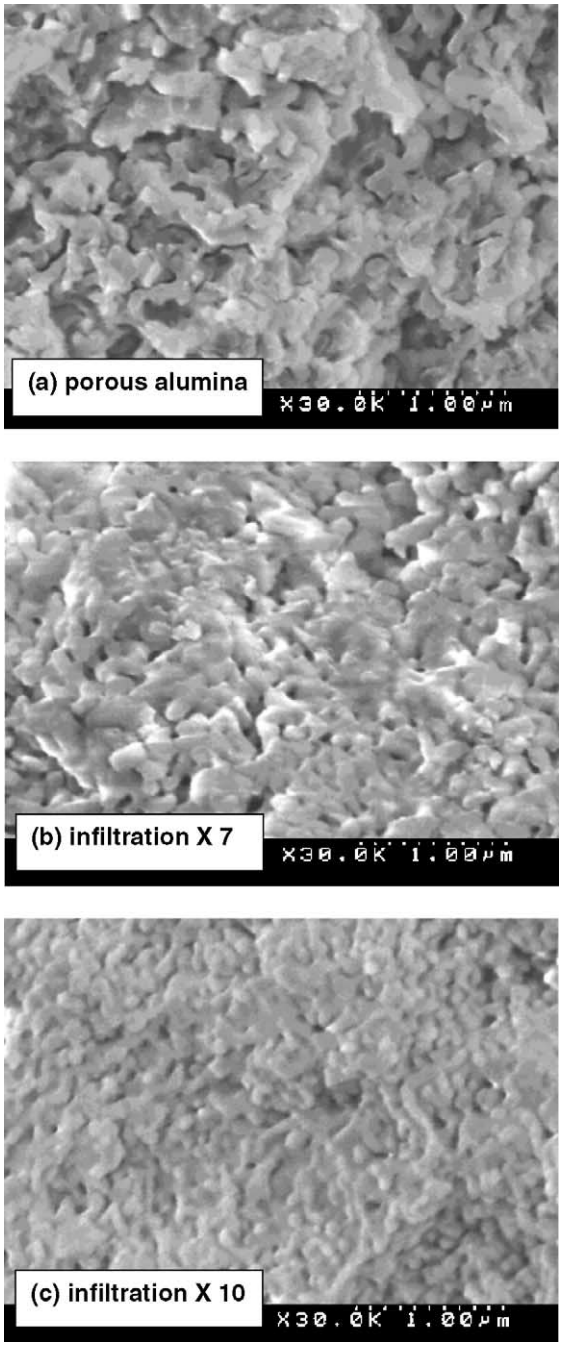

Fig. 4. Scanning electron micrographs of fabricated composite.

loss at 110–257 °C may be due to partial decomposition of perchloric acid that resides in open pores near the surface.

FT-IR patterns for the gel glass and composite are shown in Fig. 6(a). Scholze [16,17] found that there are three main IR absorption bands due to hydroxyl groups in glasses, i.e. band-1 in the range of 3640–3900 cm^{-1}, band-2 around 2900 cm^{-1}, and band-3 at 2340 cm^{-1}. The existence of the band-3 is not conformed, however, as various absorption bands due to network formers overlap in the region [16,17]. Band-1 is due to hydrogen-bond-free hydroxyl groups, and band-2 to strongly-hydrogen-bonded hydroxyl groups. It has

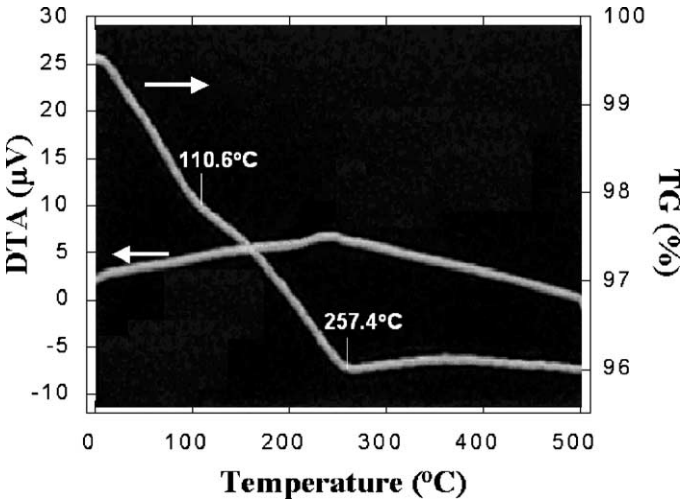

Fig. 5. DT/TGA analysis of composite.

been reported that protons in band-2 are much more mobile than those in band-1 [18]. These two bands together with an absorption peak at ~1600 cm^{-1} due to molecular water are observed in the IR patterns of both the gel and the composite. The generalized absorbance intensities of both samples are illustrated in Fig. 6(b). There is a large decrease in absorbance intensity around band-1 (about 18%) and band-2 (about 20%) in the pattern for the composite compared with that for the gel glass, while a small decrease (about 3%) by water is detected. This behavior of the composite indicates a decrease in the proton-conducting part by introducing the insulating alumina matrix.

The weight change by water absorption in the gel glass and the composite at different value of relative humidity and at 80 °C is shown in Fig. 7(a). The weights at zero relative humidity were measured using samples heat-treated at 110 °C for 2 h and then were used as criteria to plot the weight change. With increasing relative humidity up to 99 RH%, the weight of both the gel glass and the composite increased exponentially up to +33 and +16%, respectively. Nyquist plots of the composite at different levels of relative humidity are presented in Fig. 7(b). The electrical resistance of the composite decreases as the relative humidity increases, and the conductivity versus relative humidity plot is in good accordance with the weight versus relative humidity plots (Fig. 7(c)). The weight change versus relative humidity plot of the composite exhibits a pseudo-linear region at 20–99 RH% that fits the equation:

$$\log W = \left\{ \frac{\log W_2 - \log W_1}{H_{R2} - H_{R1}} \right\} H_R + \log W_0 \quad (1)$$

$$\frac{H_R}{H_{R2} - H_{R1}} = \frac{\log W}{\log W_2 - \log W_1} \quad (2)$$

where W and H_R represent the increased weight (%) and relative humidity (RH%), respectively; $\log W_0$ is the weight change at 0 RH%, that is, log 1. The proton conductivity versus weight change plot of the composite can be transformed

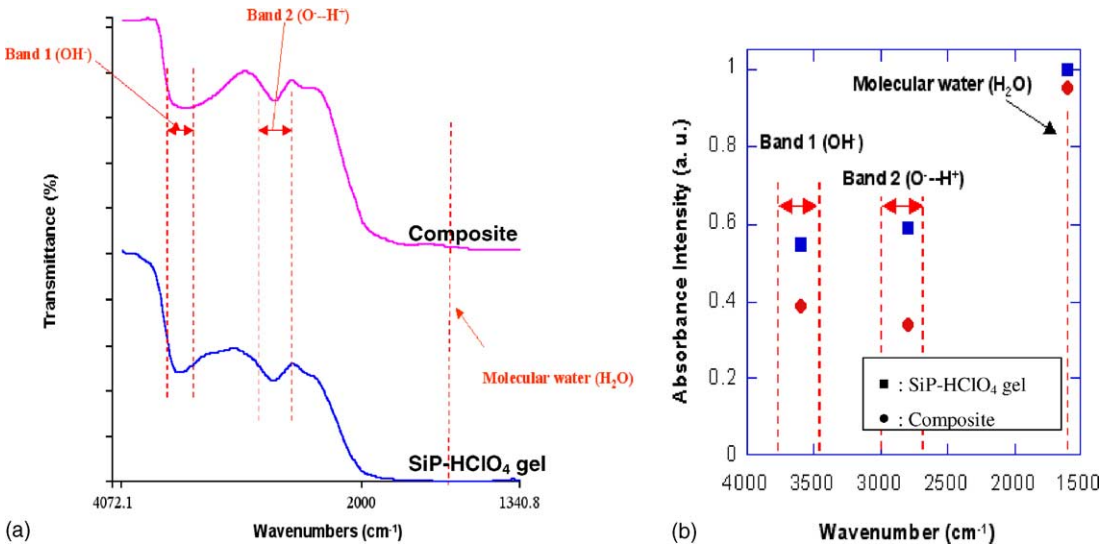

Fig. 6. (a) FT-IR patterns and (b) absorbance intensity of gel and composite.

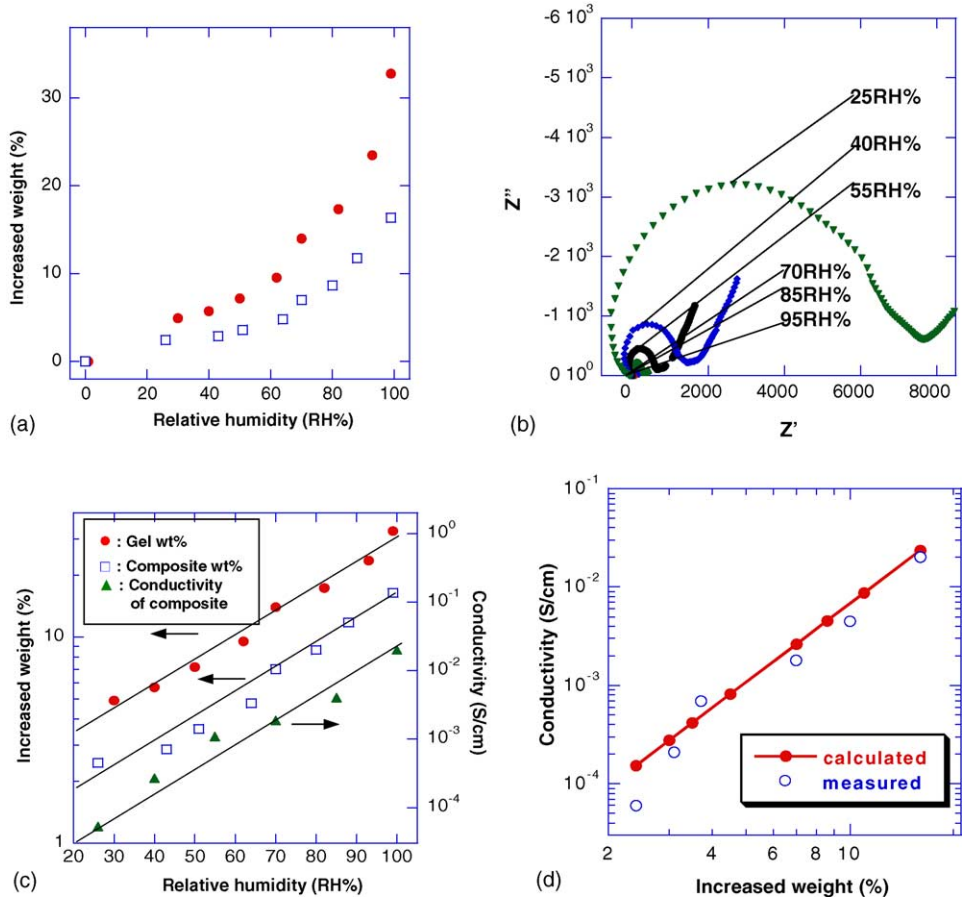

Fig. 7. (a) Weight change by water absorption; (b) Nyquist plots of composite at different relative humidities; (c) weight change and conductivity of gel glass and composite at different relative humidities ((●) SiP-$HClO_4$ gel; (□) composite; (▲) conductivity of composite); (d) calculated conductivity of composite as function of weight change ((●) calculated, (○) measured).

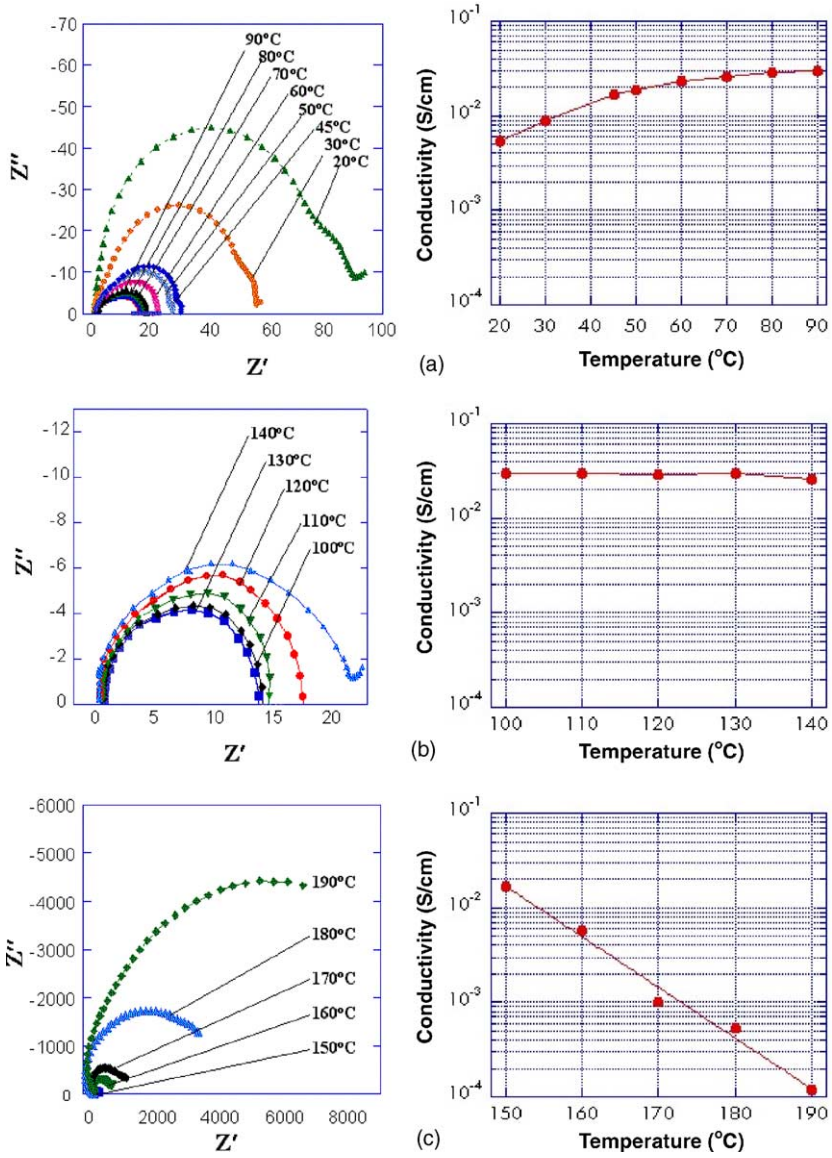

Fig. 8. Nyquist plots and calculated conductivities of composite at different temperatures: (a) 20–90 °C; (b) 100–140 °C, (c) 150–190 °C.

into a linear function of weight change by derivation from Eqs. (1) and (2):

$$\log\sigma = \left\{\frac{\log\sigma_2 - \log\sigma_1}{H_{R2} - H_{R1}}\right\} H_R + \log\sigma_0$$
$$= \frac{(\log\sigma_2 - \log\sigma_1)\log W}{\log W_2 - \log W_1} + \log\sigma_0$$
$$= a\log W + b \qquad (3)$$

where σ represents the conductivity of the composite. The value of a and b are calculated from experimental results and are 2.6552 and −4.8239, respectively. The calculated plots from Eq. (3) are well-matched with the measured conductivity of the composite, and show a large increase from 5×10^{-5} to 2×10^{-2} S cm^{-1} as the weight increases (Fig. 7(d)).

From the above results, it is clear that the weight increase of the composite is due to absorbed water, and that the water

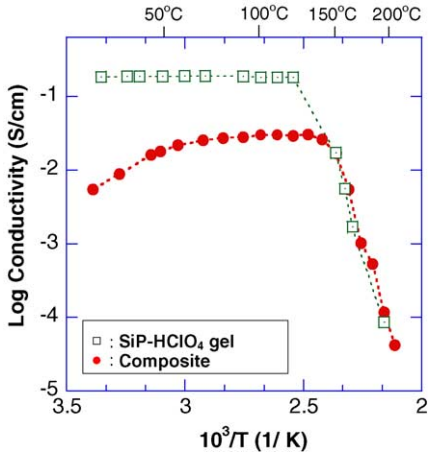

Fig. 9. Arrhenius plots of gel and composite.

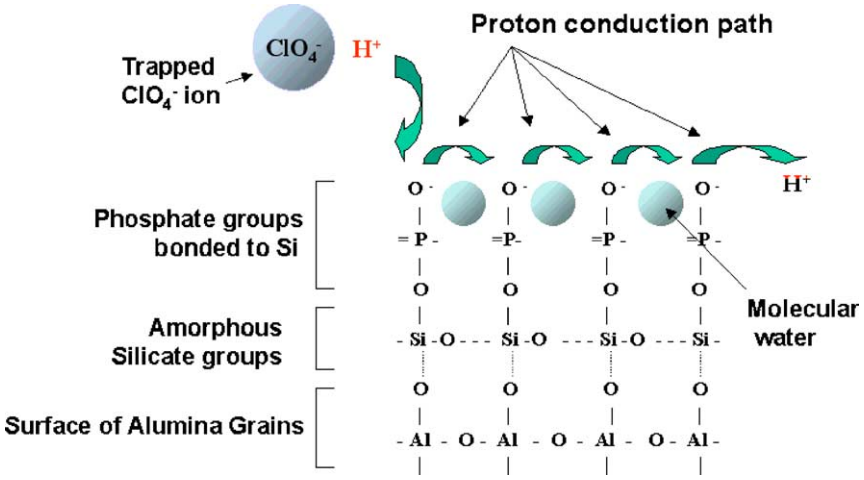

Fig. 10. Schematic diagram of proton-conduction path in molecular structure of SiP-$HClO_4$ gel glass.

directly contributes to a large increase in the proton conductivity. The high absorption ability of the gel glass is due to: (i) the formation of phosphate groups that have high reactivity with water; (ii) the mesoporous structure of the sol–gel derived gel glass and alumina substrate that has a large surface area and results in a high capillary force.

Nyquist plots and calculated conductivities of the composite at different temperature are given in Fig. 8. To make the measuring atmosphere resemble an actual MEA of a standard PEMFC stack, no pressure was engaged and the humidifier temperature was fixed at 110 °C. As the measuring temperature is increased from 20 to 90 °C, the conductivity largely increases from 5.3×10^{-3} to 2.0×10^{-2} S cm^{-1}. In the temperature range of 100–140 °C, however, the conductivity displays on a very small change, i.e. 2.6×10^{-2} to 3.0×10^{-2} S m^{-1}. Then, a large decrease of conductivity is observed as the temperature is increased further. The conductivity falls drastically from 1.06×10^{-2} to 1.04×10^{-4} S cm^{-1} on increasing the temperature from 150 to 190 °C. This decrease in conductivity is due to the fast evaporation of absorbed water that results in the breaking of proton-conducting paths and a consequent decrease in proton mobility. The conductivity of the composite exhibited good reproducibility during repeated experiments performed at 20–200 °C. Therefore, the decrease in conductivity over 140 °C is attributed to a decrease of water content, and not to thermal decomposition of the components.

Arrhenius plots of the gel glass and composite are shown in Fig. 9. The conductivity of the gel glass is about an order of magnitude larger than that of the composite over the given temperature range. The relatively low conductivity of the composite is attributed to the insulating alumina matrix. The obtained high conductivity of the gel glass indicates that proton conduction paths are successfully formed through the SiP-$HClO_4$ which contains both the trapped acid ions (ClO_4^-) as a proton source and the strongly hydrogen-bonded hydroxyl groups combined to P–O–Si bonds as proton conduction paths (Fig. 10) [19,20]. The molecular water that is contained in the gel structure also provides high proton mobility, and therefore, contributes to an increase in proton conductivity. According to Abe [20], the activation energies for the dissociation or ionization of protons in hydroxyl groups are essentially the same when the values for υ_{OH}(peak wavenumber of the IR absorption band due to fundamental O–H stretching vibration) are the same, but the activation energies for transport (proton hopping) are different. That is, the activation energy for hopping through molecular water is much less than that through non-bridging oxygen. The improved proton mobility by molecular water may be another advantage of sol–gel derived proton conducting glasses.

4. Conclusions

A high proton-conducting silicophosphate-$HClO_4$ (SiP-$HClO_4$) gel glass and a SiP-$HClO_4$–alumina composite have been successfully fabricated. The composite has high thermal stability and also high proton conductivity. The proton conductivities of the gel glass and the composite increase up to about 400-fold with increasing relative humidity. The composite shows a stable conductivity region at 100–140 °C, and indicated that the proton conductivity is over 2.6×10^{-2} S cm^{-1}. The high proton conductivity of the composite is due to the nanostructure, which contains both trapped solid acids ($HClO_4$) as a proton source and strongly hydrogen-bonded hydroxyl groups combined to P–O–Si oxide bonds as proton conduction paths. The molecular water contained in a gel structure is also considered to provide high proton mobility, which results in an increase of proton conductivity.

References

[1] R.M. Formato, P. Osenar, R.F. Kovar, DOE/ONR Fuel Cell Workshop Presentation Documents on 6–8 October, Baltimore, USA, 1999.

[2] G. Nagy, G.A. Gerhardt, A.F. Oke, R.N. Adams, R.B. Moore, M.N. Szentirmay, C.R. Martin, J. Electroanal. Chem. 188 (1985) 85.
[3] E.W. Kristensen, W.G. Khur, R.M. Wightman, Anal. Chem. 59 (1987) 1752.
[4] J. Baur, E.W. Kristensen, L.J. May, D.J. Wiedemann, R.M. Wightman, Anal. Chem. 60 (1988) 1268.
[5] D. Wiedemann, K.T. Kawagoe, R.T. Kennedy, E.L. Ciolkowski, R.M. Wightman, Anal. Chem. 63 (1987) 1965.
[6] H. Gunasingham, C. Tan, Analyst 114 (1989) 695.
[7] B. Hoyer, T.M. Florence, G.E. Bately, Anal. Chem. 59 (1987) 1608.
[8] D.J. Harrison, R.F.B. Turner, H.P. Bates, Anal. Chem. 60 (1988) 2002.
[9] E. Stolper, Contrib. Miner. Petrl. 81 (1982) 1.
[10] E.N. Boulos, N.J. Kreidl, J. Can. Ceram. Soc. 41 (1972) 83.
[11] K. Kawamura, H. Hosono, H. Kawazoe, N. Matsunami, Y. Abe, J. Jpn. Ceram. Soc. 104 (1996) 688.
[12] H. Namikawa, Y. Asahara, J. Jpn. Ceram. Soc. 74 (1966) 205.
[13] H. Hosono, T. Kamae, Y. Abe, J. Am. Ceram. Soc. 72 (1989) 294.
[14] Y. Abe, G. Li, M. Nogami, T. Kasuga, J. Electrochem. Soc. 143 (1996) 144.
[15] M. Nagai, T. Nishino, Key Eng. Mater. 111–112 (1995) 28.
[16] Y. Abe, G. Li, M. Nogami, T. Kasuga, J. Electrochem. Soc. 143 (1) (1996) 144.
[17] H. Scholze, Glastech. Ber. 32 (1959) 142.
[18] E.N. Boulos, N.J. Kreidl, J. Can. Ceram. Soc. 41 (1972) 83.
[19] Y.-I. Park, J.-D. Kim, M. Nagai, J. Mater. Sci. Lett. 19 (2000) 2251.
[20] Y. Abe, Proc. XVII Int. Congr. Glasses 1 (1995) 105.